Analytical Model for a Cylinder Sinking Into a Thin Film

by

Kevin T. Chen

Submitted to the Department of Mechanical Engineering
in partial fulfillment of the requirements for the degree of

Bachelor of Science in Mechanical Engineering

at the

MASSACHUSETTS INSTITUTE OF TECHNOLOGY

June 2005

Author .....

Department of Mechanical Engineering
May 6, 2005

Certified by .....

Anette E. Hosoi
Assistant Professor
Thesis Supervisor

Accepted by .....

Ernest G. Cravalho
Chairman of Undergraduate Thesis Committee

Analytical Model for a Cylinder Sinking Into a Thin Film

by

Kevin T. Chen

Submitted to the Department of Mechanical Engineering
on May 6, 2005, in partial fulfillment of the
requirements for the degree of
Bachelor of Science in Mechanical Engineering

Abstract

New technologies and techniques have enabled oil companies to access oil deposits by drilling through the ground horizontally. These increased capabilites have improved drilling efficiencies, and have also reduced the effects that drilling has on the local environment. These boreholes can be enormously long, and it is often necessary to send a tethered robot into the hole in order to gather information. If these robots remain stationary for too long, however, their tethering cables can become stuck in the mud cake lining the walls. The recovery or replacement of these robots is time consuming and expensive, so it is desirable to understand how and why the cables sink. In this analysis, the mud cake is modeled as a Newtonian fluid. The surface of the cable is approximated as being either parabolic or circular, and it is shown that the sinking is governed by exactly two dimensionless parameters in both cases. Matlab is used to visualize the evolution of the fluid pressure distribution with time, as well as the time it takes for the cylinder to settle to 20 percent of the mud cake thickness.

Thesis Supervisor: Anette E. Hosoi
Title: Assistant Professor

Acknowledgments

Special thanks to Peko Hosoi, Julio Guerrero, and Debra Blanchard for all of their thoughtful help.

Contents

List of Figures

Chapter 1

Introduction

1.1 Motivation

Recent advances in oil drilling technology have enabled oil companies to bore horizontally through bedrock in order to access oil deposits. This reduces the environmental impact of drilling, as it gives the drillers more flexibility in selecting their drilling sites. With this added flexibility, oil deposits located directly below environmentally sensitive areas can be tapped without negative effects to the land above. In addition, multiple horizontal branches can be drilled from a single hole, which reduces the overall number of holes that must be drilled.

In order to drill such deep holes, oil companies must use specially designed hollow drill bits. Drilling mud is pumped through the drill string, and it flows out through holes in the drill bit. This mud lubricates the bit as it cuts through the bedrock, then carries sediment and debris from the drilling up to the surface. For horizontal drilling, the drill bit is attached to a steerable downhole motor, which allows operators to adjust the angle of the bit as it drills. Current technology enables drillers to change the angle of a well up to 110 degrees within just a few hundred feet, and horizontal holes have been drilled to lengths of over 35,000 feet [4].

When drilling of the well has ceased, a remote-controlled robot is sent into the hole on a steel cable tether to gather data about the well. These wells, however, are usually several thousand feet deep, and temperatures and pressures at the bottoms of

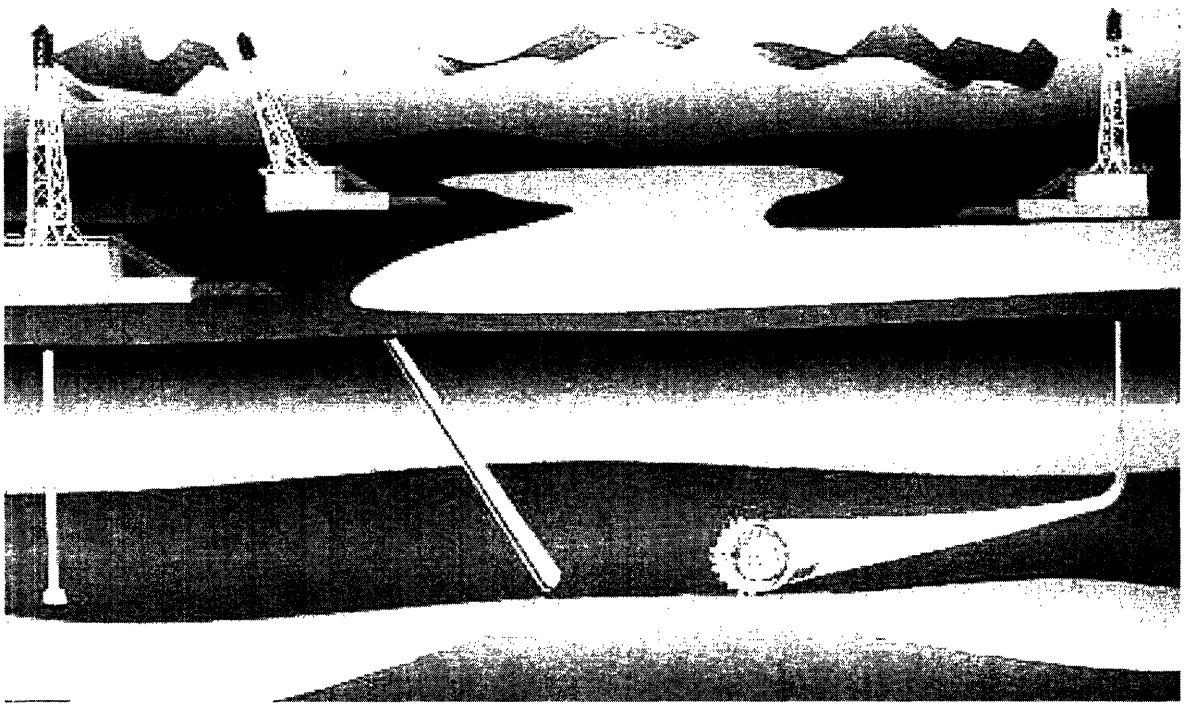

Figure 1-1: Comparison of drilling strategies (taken from OTS Heavy Oil Science Centre website)

the wells can be enormous (300-500 degrees F, and 20,000 psi). Although the pressure is naturally high due to hydrostatic pressure, drillers typically keep the mud-filled holes artificially pressurized in order to prevent the walls from collapsing. Such high pressures force the mud to leach into the dirt covered walls of the well, forming a thin, viscous mud cake layer between the mud and the bedrock. If left to settle, the robot's tether cable can sink into this layer of mud cake; after about 20 minutes, the cable is unmovable. The cost of either recovering or replacing the robot is enormous, so gaining a thorough understanding about how the cylinder sinks is of great interest to oil companies.

1.2 Scope of Analysis

The mud cake can be modeled as a Bingham fluid. In a Bingham fluid, the fluid does not shear until it reaches a certain yield stress, above which it behaves as a Newtonian fluid. As a first-order approximation, this analysis models the problem as

an infinite cylinder sinking onto an infinite plane, with the mud cake approximated as a thin film of Newtonian fluid. In this case, it is shown that the sinking of the cylinder is governed by exactly two dimensionless parameters, whether the surface of the cylinder is approximated as parabolic or circular.

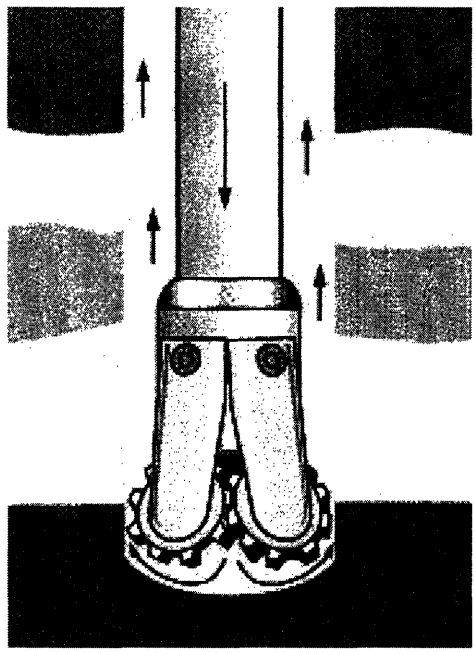

Figure 1-2: Example of an oil drill bit (taken from HowStuffWorks.com)

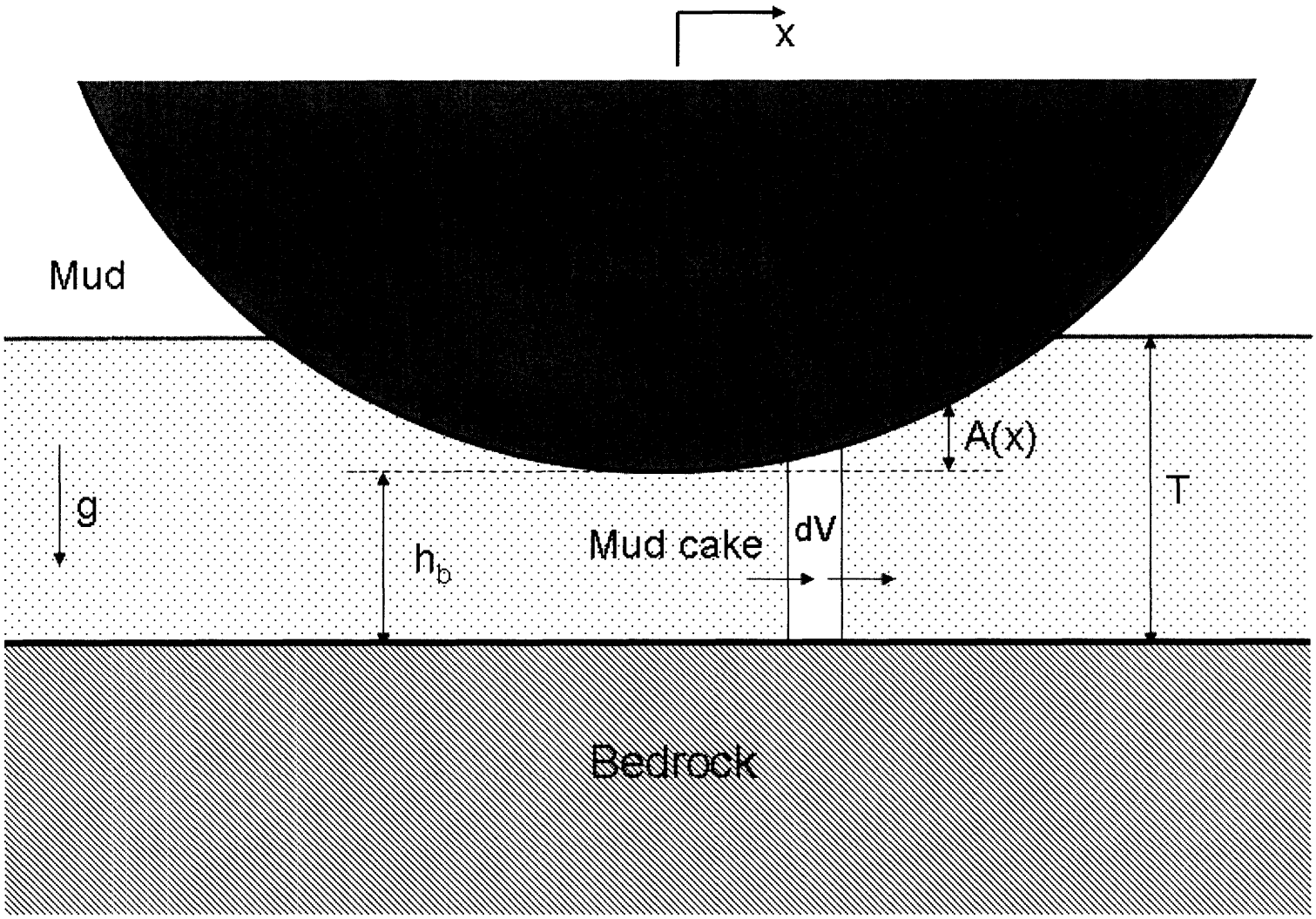

Figure 1-3: Illustration of the sinking cylinder model

Chapter 2

Derivation

2.1 General Case for Newtonian Fluid

The steel cable typically has a diameter of about one inch, whereas the diameter of the oil well is usually six to twelve inches. Because the diameter of the cable is significantly smaller than that of the well, the curvature of the well can be neglected, and the problem can be approximated as a cylinder sinking on a flat surface (see Figure 1.3).

Furthermore, because the thickness of the mud cake is very small (usually about a quarter of an inch), the lubrication approximation can be used. This implies that the fluid velocity is small in the vertical direction, and that the pressure is a function only of x (horizontal position) and t (time). In the first part of the analysis, the mud cake is modeled as a Newtonian fluid.

Using the lubrication approximation and imposing the no-slip boundary condition at the bedrock ($y = 0$) and at the cylinder ($y = h$), one can find an analytical expression for the velocity in the x-direction (see Appendix B),

$$u(x, y, t) = \left(\frac{1}{2\mu}\right)\left(\frac{\partial p}{\partial x}\right)(y^2 - hy), \tag{2.1}$$

where the surface of the cylinder, h, is given by

$$h(x,t) = h_b(t) + A(x), \tag{2.2}$$

where $h_b(t)$ represents the position of the bottom of the cylinder as a function of time, and $A(x)$ represents the geometric shape of the cable. In this analysis, parabolic and circular profiles are examined.

Imposing a simple mass balance on a differential control volume under the sinking cylinder, one can derive the expression

$$\frac{\partial h}{\partial t} - \frac{1}{12\mu} \cdot \frac{\partial}{\partial x}\left(\frac{\partial p}{\partial x} h^3\right) = 0. \tag{2.3}$$

Because only the h_b portion of the expression for h varies with time, Equation 2.3 is rewritten as

$$\frac{\partial h_b}{\partial t} - \frac{1}{12\mu} \cdot \frac{\partial}{\partial x}\left(\frac{\partial p}{\partial x} h^3\right) = 0. \tag{2.4}$$

The $\frac{\partial p}{\partial x}$ term can be found by performing a force balance on the cylinder. Gravity pulls the cylinder downwards while the fluid pressure pushes the cylinder upwards, and inertial effects can be ignored because the cylinder sinks very slowly. An expression for this resistance caused by fluid pressure can be determined from the dot product of fluid stress tensor and the normal vector to the cylinder surface. The fluid stress tensor for a thin film of a Newtonian fluid, τ_{ij}, is

$$\tau_{ij} = \begin{pmatrix} -p & \mu\frac{\partial u}{\partial y} \\ \mu\frac{\partial u}{\partial y} & -p \end{pmatrix},$$

and the unit normal vector to the cylinder surface, $\vec{n}$, is

$$\vec{n} = \left(-\frac{\partial h}{\partial x}, 1\right) \cdot \frac{1}{\sqrt{1 + \left(\frac{\partial h}{\partial x}\right)^2}}. \tag{2.5}$$

The dot product of these two expressions then, is the force exerted on the fluid by the sinking cylinder. As the x-component of this force cancels due to symmetry,

the only component of interest is the vertical force,

$$\vec{F_y} = \left[-p - \mu \cdot \frac{\partial h}{\partial x} \cdot \frac{\partial u}{\partial y}\right] \cdot \frac{1}{\sqrt{1 + \left(\frac{\partial h}{\partial x}\right)^2}}. \tag{2.6}$$

The overall force on the cylinder can be calculated by reversing the sign of Equation 2.6 to represent the vertical force exerted on the cylinder by the fluid, then integrating over the area of the cylinder in contact with the fluid. For a cylinder of unit length, the expression becomes

$$\frac{mg}{W} = \int_S \left[\frac{1}{2} \cdot \frac{\partial h}{\partial x} \cdot \frac{\partial p}{\partial x} \cdot h + p\right] \cdot \frac{1}{\sqrt{1 + \left(\frac{\partial h}{\partial x}\right)^2}} dS, \tag{2.7}$$

where m is the overall mass of the cable, W is the overall length of the cable, and g is the gravitational constant. This can be rewritten as

$$\frac{mg}{W} = 2 \cdot \int_0^{x_m} \left[\frac{1}{2} \cdot \frac{\partial h}{\partial x} \cdot \frac{\partial p}{\partial x} \cdot h + p\right] dx. \tag{2.8}$$

In the above expression, x_m represents the maximum value of x at which the surface of the cylinder is in contact with the mud cake. It is clear, then, that x_m increases as the cylinder sinks.

Using this vertical force balance (Equation 2.8) along with the differential mass conservation equation (Equation 2.4), the height of the cylinder as a function of time can be found. In order to obtain an analytically solvable set of equations, we use a collocation method. To do this, the pressure p can be approximated as a second-order polynomial, namely

$$p(x,t) = p_0(t) + p_1(t)x + p_2(t)x^2. \tag{2.9}$$

Since the pressure must be horizontally symmetrical with respect to the cylinder, however, the p_1 term must equal zero, which yields the simpler expression:

$$p(x,t) = p_0(t) + p_2(t)x^2. \tag{2.10}$$

Furthermore, the value of the pressure, p, must approach the ambient pressure as the horizontal distance from the cylinder increases. If this ambient pressure is defined to be zero, then the pressure boundary condition that $p = 0$ when $x = x_m$ can be imposed. This produces an expression for p_0 in terms of x_m:

$$p_0 = -p_2 x_m^2. \tag{2.11}$$

Incorporating these constitutive relations for the pressure, the preceding equations can then be solved by using a Euler time step. Also, this analysis focuses on a very small area directly below the cylinder, so it is valid to evaluate this expression at a Gauss point of $x = 0$ to simplify the expression. Assuming some initial condition, the following discretized version of Equation 2.4 can be used to solve for h_b^{n+1}:

$$\frac{h_b^{n+1} - h_b^n}{\Delta t} = \frac{p_2^n (h_b^n)^3}{6\mu}, \tag{2.12}$$

where h^n refers to the current height, and h^{n+1} refers to the height after the next time step.

Using h_b^{n+1} as a new initial condition, one can then recalculate the value of p_2, which will yield the next value of h_b. After repeated iterations, this process eventually determines the overall change in h_b with time.

2.2 Parabolic geometry

As a first approximation, the profile of the cylinder can be approximated as a parabola. This means that the height of the cylinder, $h(x,t)$, can be written as

$$h(x,t) = h_b(t) + kx^2. \tag{2.13}$$

This, in turn, leads to the following expression for the force in the y-direction:

$$\vec{F_y} = 2 \cdot \int_0^{x_m} \left[kx \left(\frac{\partial p}{\partial x} \right) (h_b + kx^2) + p \right] dx. \tag{2.14}$$

where x_m can now be calculated as

$$x_m = \sqrt{\frac{T - h_b}{k}}. \tag{2.15}$$

Again, x_m simply represents the maximum value of x at which the surface of the cylinder is still in contact with the mud cake layer. Now, substituting this expression back into the y-direction force balance (Equation 2.14) and integrating, the force balance equation becomes:

$$\frac{mg}{W} = \frac{4}{5}k^2 x_m^5 p_2 + \frac{2}{3}k h_b x_m^3 p_2 - \frac{2}{3}x_m^3 p_2. \tag{2.16}$$

The constitutive relations between p_0, p_2 (2.11) and the expression for x_m (2.15) can be used to eliminate p_0 and x_m from the above equation, which leaves only p_2 and h_b as unknowns. Assuming some initial value for h_b, the value of p_2 then can be found analytically.

It is also helpful to non-dimensionalize the above equations so that the resulting data are scalable to a variety of different physical parameters. The relevant variables are scaled as follows:

$$y = T\tilde{y} \tag{2.17}$$

$$x = \frac{1}{k}\tilde{x} \tag{2.18}$$

$$h_b = T\tilde{h}_b \tag{2.19}$$

$$t = \sqrt{\frac{T}{g}}\tilde{t} \tag{2.20}$$

$$p = \frac{\mu}{\sqrt{T}g}\tilde{p} \tag{2.21}$$

$$p_2 = \frac{\mu k^2 \sqrt{g}}{\sqrt{T}}\tilde{p}_2 \tag{2.22}$$

Using the above scaling, an analytical expression for $\tilde{p}_2$ can be found as

$$\tilde{p}_2 = \frac{km\sqrt{gT}}{\mu W}\left(\frac{4}{5}\tilde{x}_m^5 + \frac{2}{3}Tk\tilde{x}_m^3 - \frac{2}{3}\tilde{x}_m^3\right)^{-1}, \tag{2.23}$$

where

$$\tilde{x}_m = \sqrt{Tk(1-\tilde{h}_b)}. \tag{2.24}$$

Once the value for $\tilde{p}_2$ is known, the dimensionless mass balance relation,

$$\frac{\tilde{h}_b^{n+1} - \tilde{h}_b^n}{\Delta\tilde{t}} = \frac{T^2k^2}{6}\tilde{p}_2(\tilde{h}_b^n)^3, \tag{2.25}$$

can be used to determine the change in $\tilde{h}_b$ with time.

2.3 Circular geometry

A more accurate expression for the profile of the cylinder surface is a circle. This means that the height of the cylinder above the bedrock must be written as

$$h(x,t) = h_b + R - \sqrt{R^2 - x^2}. \tag{2.26}$$

Integrating the pressure across the lower surface of the cylinder, an expression for the force exerted on the cylinder by the fluid can be found as

$$\vec{F}_y = 2 \cdot \int_0^{x_m} \left[\left(\frac{x}{2\sqrt{R^2-x^2}}\right)\left(\frac{\partial p}{\partial x}\right)\left(h_b + R - \sqrt{R^2-x^2}\right) + p\right] dx, \tag{2.27}$$

where x_m is now written as

$$x_m = \sqrt{R^2 - (T - h_b - R)^2}. \tag{2.28}$$

Again, this fluid pressure force can be balanced with the force of gravity and combined with various constitutive relations to yield an expression for p_2,

$$p_2 = \frac{mg}{W}\left[(h_b + R)\left(R^2 \sin^{-1}\left(\frac{x_m}{R}\right) - x_m\sqrt{R^2 - x_m^2}\right) - 2x_m^3\right]^{-1}. \tag{2.29}$$

It is helpful again to non-dimensionalize the governing equations in order to make them easily scalable. The parameters can be scaled with the same factors as in the parabolic case, only using $x = R\tilde{x}$ in place of $x = \frac{1}{k}\tilde{x}$. This yields an expression for the non-dimensional $\tilde{p}_2$ as

$$\tilde{p}_2 = \frac{m\sqrt{gT}}{\mu W R}\left[\left(\frac{T}{R}\tilde{h}_b + 1\right)\left(\sin^{-1}(\tilde{x}_m) - \tilde{x}_m\sqrt{1 - \tilde{x}_m^2}\right) - 2\tilde{x}_m^3\right]^{-1}, \tag{2.30}$$

where $\tilde{x}_m$ can be written as

$$\tilde{x}_m = \sqrt{2 - \frac{T^2}{R^2}(1 - \tilde{h}_b)^2 + 2\frac{T}{R}(1 - \tilde{h}_b)}. \tag{2.31}$$

Once $\tilde{p}_2$ is found for a given $\tilde{h}_b$, it can be plugged into the non-dimensional mass balance,

$$\frac{\tilde{h}_b^{n+1} - \tilde{h}_b^n}{\Delta\tilde{t}} = \frac{T^2}{6R^2}\tilde{p}_2(\tilde{h}_b^n)^3, \tag{2.32}$$

to determine the evolution of $\tilde{h}_b$ with time.

Chapter 3

Analysis

3.1 Parabolic Geometry

The non-dimensionalized equations for $\tilde{p}_2$ and $\tilde{h}_b$ appear to be extremely complicated, but actually depend only on two dimensionless parameters,

$$\Pi_1 = \frac{km\sqrt{gT}}{\mu W}, \tag{3.1}$$

and

$$\Pi_2 = Tk. \tag{3.2}$$

As such, Equation 2.23 can be rewritten as

$$\tilde{p}_2 = \Pi_1 \left(\frac{4}{5}\tilde{x}_m^5 + \frac{2}{3}\Pi_2 \tilde{x}_m^3 - \frac{2}{3}\tilde{x}_m^3 \right)^{-1}, \tag{3.3}$$

where

$$\tilde{x}_m = \sqrt{\Pi_2(1 - \tilde{h}_b)}. \tag{3.4}$$

Equation 2.25 then becomes

$$\frac{\tilde{h}_b^{n+1} - \tilde{h}_b^n}{\Delta\tilde{t}} = \frac{\Pi_2^2}{6}\tilde{p}_2(\tilde{h}_b^n)^3. \tag{3.5}$$

If typical physical parameters for the system are used, and the initial position of the cylinder is $\tilde{h}_b = 0.4$, then the variation of non-dimensional pressure with $\tilde{x}$ and $\tilde{t}$ looks like:

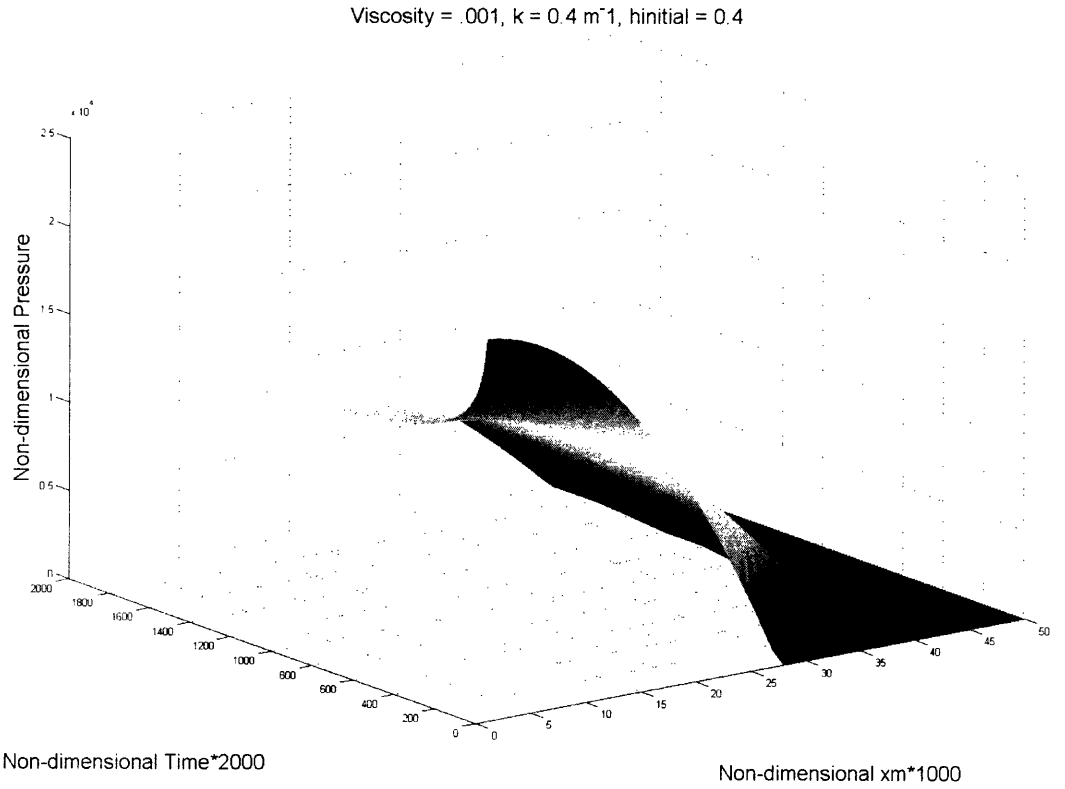

Figure 3-1: Change in $\tilde{p}$ with time

The change in the cylinder height with time looks like:

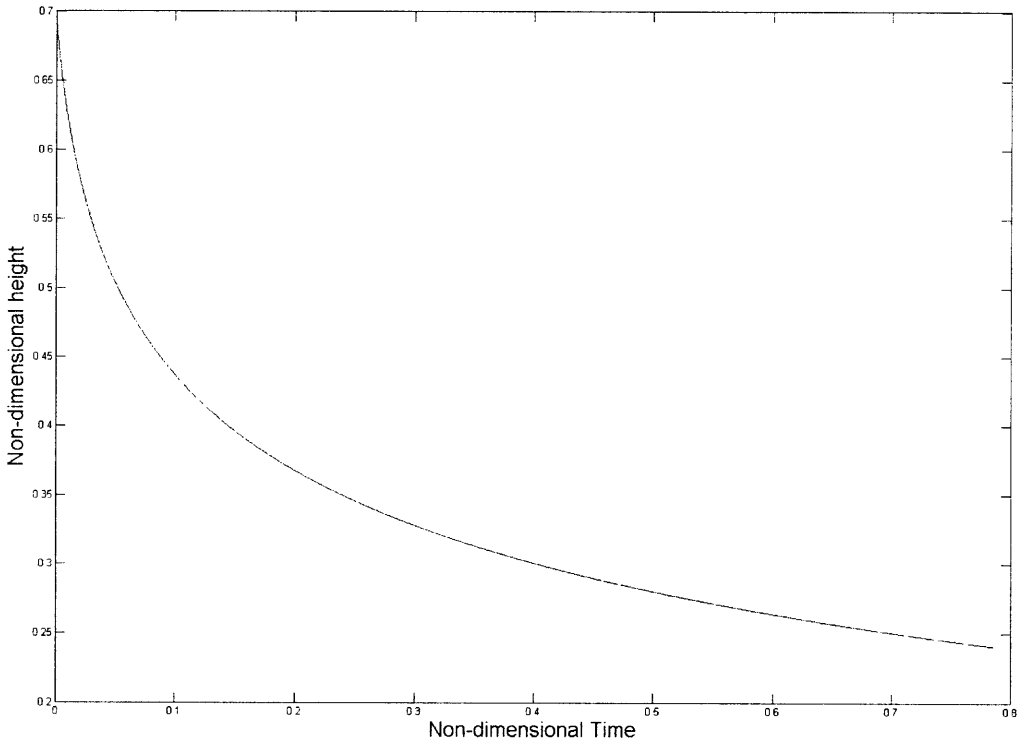

Figure 3-2: Change in $\tilde{h}_b$ with time

3.2 Circular Geometry

As with the parabolic geometry, the seemingly complicated expressions for $\tilde{p}_2$ and $\tilde{h}_b$ with circular geometry depend on just two dimensionless parameters. The parameters for the circular geometry are very similar to the parabolic parameters, and are defined as

$$\Pi_1 = \frac{m\sqrt{gT}}{\mu WR}, \tag{3.6}$$

and

$$\Pi_2 = \frac{T}{R}. \tag{3.7}$$

Using these Π-groups in Equations 2.30, 2.31, and 2.32 respectively,

$$\tilde{p}_2 = \Pi_1 \left[\left(\Pi_2 \tilde{h}_b + 1 \right) \left(\sin^{-1}(\tilde{x}_m) - \tilde{x}_m \sqrt{1 - \tilde{x}_m^2} \right) - 2\tilde{x}_m^3 \right]^{-1}, \tag{3.8}$$

$$\tilde{x}_m = \sqrt{2 - \Pi_2^2 (1 - \tilde{h}_b)^2 + 2\Pi_2 (1 - \tilde{h}_b)}, \tag{3.9}$$

and

$$\frac{\tilde{h}_b^{n+1} - \tilde{h}_b^n}{\Delta \tilde{t}} = \frac{\Pi_2^2}{6} \tilde{p}_2 (\tilde{h}_b^n)^3, \tag{3.10}$$

It is interesting to note that the mass balance equations for both geometries are identical (Equations 3.5 and 3.10), differing only in the definition of their respective Π-groups.

Assuming similar values to those in the parabolic case, but also that $R = 0.5$ inches, the variation in $\tilde{p}$ with x and t looks like:

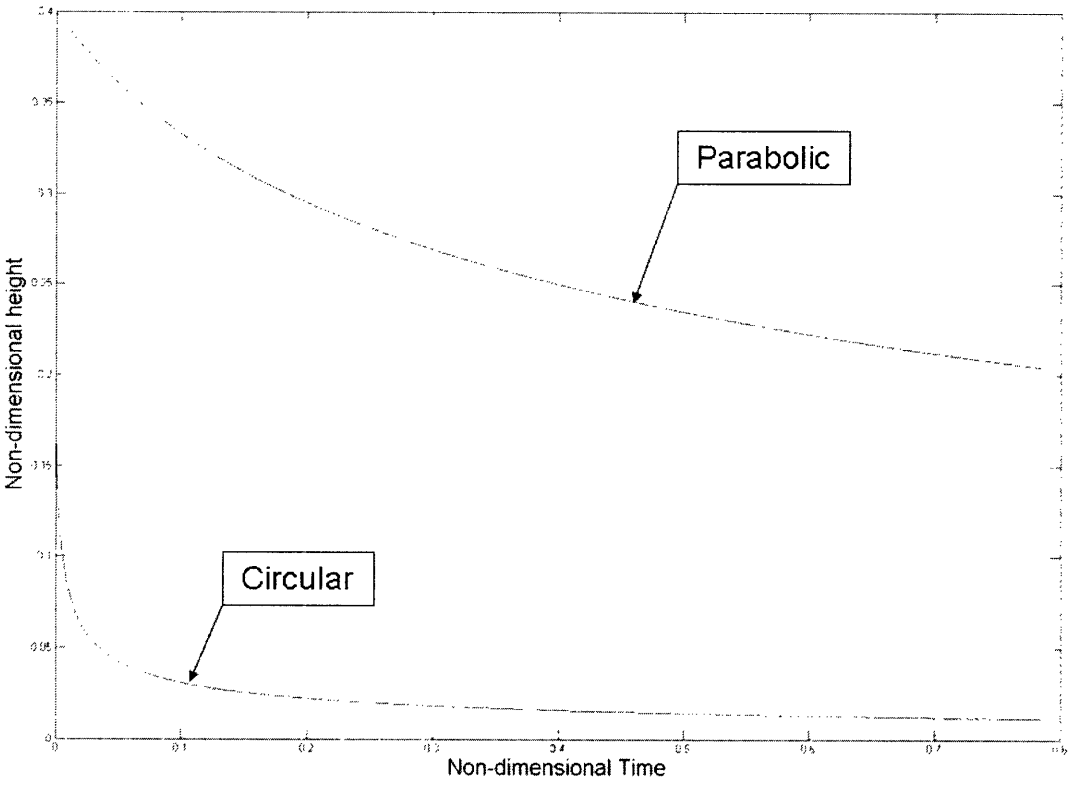

Figure 3-3: Change in $\tilde{p}$ with time

The variation of $\tilde{h}_b$ with t looks like:

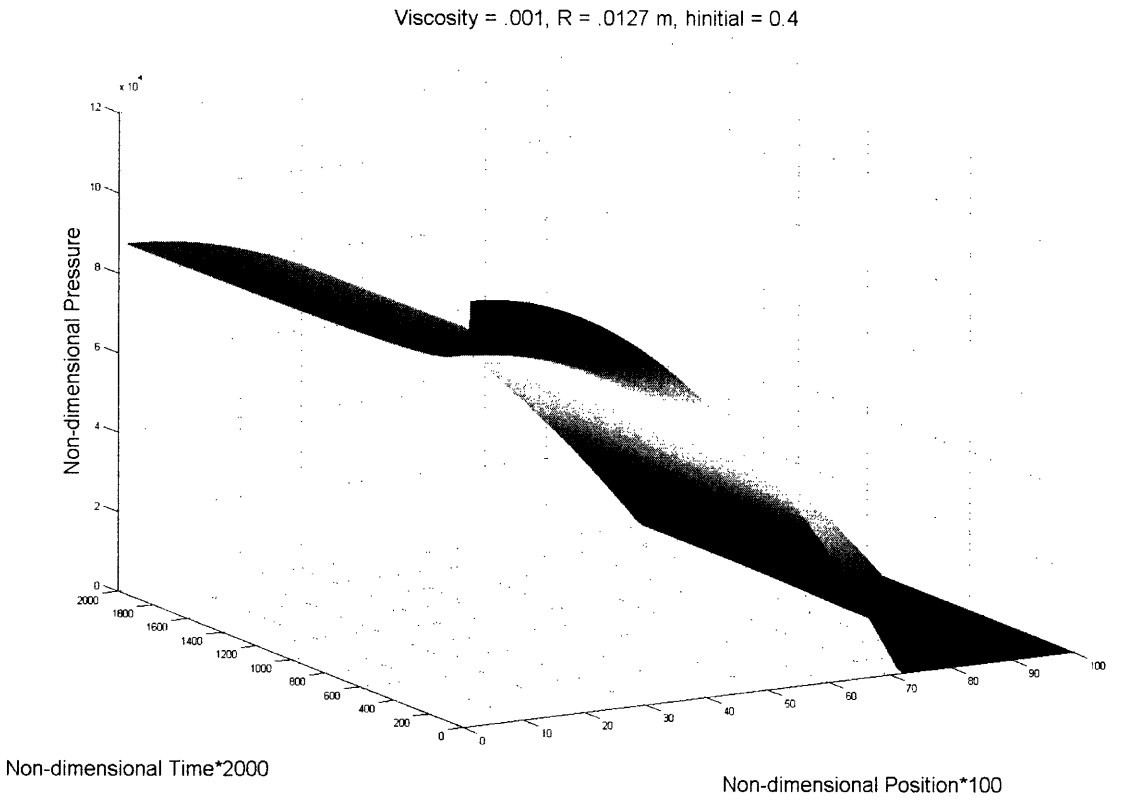

Figure 3-4: Change in $\tilde{h}_b$ with time

It is also interesting to examine the time it takes for the cylinder to sink to the point where $\tilde{h}_b = 0.2$, or 20 percent of the mud cake thickness. The following figure displays these points for a range of Π_1 and Π_2 values.

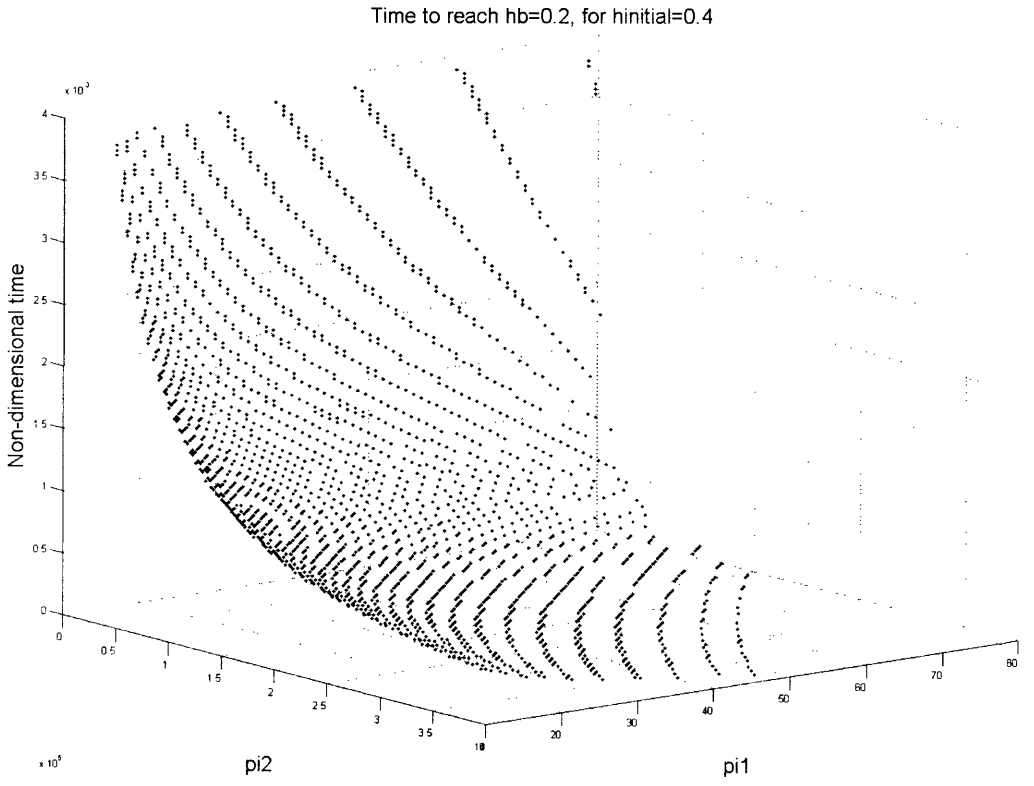

Figure 3-5: Time to reach $\tilde{h}_b = 0.2$ with respect to Π_1 and Π_2 for an initial $\tilde{h}_b = 0.4$

Appendix A

List of symbols used

$\vec{F_y}$ = vertical component of force exerted on cylinder

g = gravitational constant

h = distance between ground and surface of cylinder

h_b = distance between ground and lowest point of cylinder surface

k = parabolic scaling constant, units of 1/meter

μ = fluid viscosity

p = fluid pressure

p_0 = pressure scaling constant, $f(t)$, units of pressure

p_2 = pressure scaling constant, $f(t)$, units of pressure/square meters

Π = dimensionless parameter

R = radius of cylinder

t = time

T = thickness of the mud cake layer

τ_{ij} = stress tensor

u = horizontal component of fluid velocity

v = vertical component of fluid velocity

W = length of the cylinder (z-direction)

x = horizontal position, where $x = 0$ corresponds to center axis of cylinder

x_m = maximum value of x at which cylinder surface is in contact with mud cake

y = vertical position, where $y = 0$ corresponds to top surface of bedrock

Appendix B

Derivation of Fluid Velocity

The vertical distance between the cable and the bedrock is small compared to the horizontal span of the system, therefore the lubrication approximation can be used. This means that it is valid to assume that the pressure does not vary in the vertical direction,

$$\frac{\partial p}{\partial y} = 0, \tag{B.1}$$

and that the vertical component of the fluid velocity is negligible,

$$v \approx 0. \tag{B.2}$$

With these assumptions, the relationship between pressure and velocity,

$$\frac{\partial p}{\partial x} = \mu \left(\frac{\partial^2 u}{\partial y^2} \right), \tag{B.3}$$

can be integrated twice to yield the following expression:

$$u = \frac{1}{2\mu} \cdot \frac{\partial p}{\partial x} \cdot y^2 + Ay + B. \tag{B.4}$$

A and B are integration constants that can be found using boundary conditions. These no-slip boundary conditions simply state that the fluid velocities at the bedrock and at the surface of the cable are both zero, or

$$u|_{h=0} = 0, \tag{B.5}$$

and

$$u|_{h=h} = 0. \tag{B.6}$$

Imposing these boundary conditions yields the following expression for the fluid velocity:

$$u(x, y, t) = \left(\frac{1}{2\mu} \cdot \frac{\partial p}{\partial x}\right) \cdot (y^2 - hy). \tag{B.7}$$

Appendix C

Matlab Code

C.1 Parabolic geometry

```
%4/5/05, modified 4/19/05
%Non-dimensionalized equations
%h = hb + k*x^2

clear all;

k = .4; %parabolic shape constant
T = .00635; %in m
g = 9.81;
mu = 0.001; %in Pa-s
m = 3.98; %in kg

%hb ~ T*hb
%x ~ x/k
%p ~ p*mu/sqrt(T/g)
%p2 ~ p2*mu/k^2sqrt(T/g)

hb = 0.7; %set initial condition
```

```
hn = hb;
deltat = .00001/sqrt(T/g); %set time step amount

maxxm = round(1000*sqrt(T*k)); %maximum value of 1000*xm

for (i=1:2000) %i represents time step

    hb = hn;

    xm = sqrt(T*k*(1-hb));

    p2 = k*m*sqrt(g*T)/mu/(4/5*xm^5 + 2/3*T*k*hb*xm^3 - 2/3*xm^3);

    hn = T^2*k^2/6*p2*hb^3*deltat + hb;

    hlist(i) = hn;
    p2list(i) = p2;
    p0list(i) = -p2 * xm^2;

    for (j = 1:maxxm) %j represents x step

        if (j/1000 <= xm)
            plist(i,j) = -p2*xm^2 + p2*(j/1000)^2;

        else
            plist(i,j)=0;

        end

    end
```

```
end

t = [0:deltat:deltat*2000-deltat]; %nondimensional time
%t = [0:.00001:.01999]; %dimensional time
x = [0:.001:.036];

figure(1);
plot(t,hlist);
xlabel('Non-dimensional Time');
ylabel('Non-dimensional height');

figure(2);
plot(t,p0list);
xlabel('Non-dimensional Time');
ylabel('Non-dimensional p0');

figure(3);
plot(t,p2list);
xlabel('Non-dimensional Time');
ylabel('Non-dimensional p2');

figure(4);
surf(plist);
ylabel('Non-dimensional Time*2000');
xlabel('Non-dimensional xm*1000');
zlabel('Non-dimensional Pressure');
```

C.2 Circular geometry

```
%4/28/05
%Non-dimensionalized equations
%h = hb + R - sqrt(R^2-x^2)
%variable Gauss point

clear all;

R = .0127; %radius of cylinder, in m
T = .00635; %thickness of mud cake, in m
g = 9.81;
mu = 0.001; %viscosity, in Pa-s
m = 3.98; %mass of cylinder per unit length, in kg

%hb ~ T*hb
%x ~ R*x
%p ~ p*mu/sqrt(T/g)
%p2 ~ p2*mu*R^2sqrt(T/g)

hb = 0.4; %set initial condition
hn = hb;
deltat = .000001/sqrt(T/g); %set time step amount

W = 1; %unit length of cylinder
xg = 0; %Gauss point

maxxm = 100; %maximum value of 10000*xm

for (i=1:2000) %i represents time step
```

```
    hb = hn;

    xm = 1/R*sqrt(R^2 - (T-T*hb-R)^2);

    p2 = m*sqrt(g*T)/2/mu/R/((T/R*hb+1)*(-xm/2*sqrt(1-xm^2)+1/2*asin(xm))-xm^3);

    hn = R/6/T*p2*((T/R*hb+1-sqrt(1-xg^2))^3 - 3*xg^2*(T/R*hb+1-sqrt(1-xg^2))^2/sqrt(

    xmlist(i) = xm;
    hlist(i) = hn;
    p2list(i) = p2;
    p0list(i) = -p2 * xm^2;

    for (j = 1:maxxm) %j represents x step

        if (j/100 <= xm)
            plist(i,j) = p0list(i) + p2*(j/100)^2;

        else
            plist(i,j)=0;

        end

    end

end

t = [0:deltat:deltat*2000-deltat]; %nondimensional time
%t = [0:.0001:.1999]; %dimensional time
```

```
figure(1);
plot(t,hlist);
xlabel('Non-dimensional Time');
ylabel('Non-dimensional height');

figure(2);
plot(t,p0list);
xlabel('Non-dimensional Time');
ylabel('Non-dimensional p0');

figure(3);
plot(t,p2list);
xlabel('Non-dimensional Time');
ylabel('Non-dimensional p2');

figure(4);
surf(plist);
ylabel('Non-dimensional Time*2000');
xlabel('Non-dimensional Position*100');
zlabel('Non-dimensional Pressure');
title('Viscosity = .001, R = .0127 m, hinitial = 0.4');
```

Bibliography

[1] I.S. Gradshteyn, I.M. Ryzhik, and Alan Jeffrey. *Table of Integrals, Series, and Products.* Academic Press: 4th Edition, 1965.

[2] J. Happel and H. Bremer. *Low Reynolds Number Hydrodynamics.* Prentice-Hall, 1965.

[3] Ko Fei Liu and Chiang C. Mei. 1989. Slow spreading of a sheet of Bingham fluid on an inclined plane. *Journal of Fluid Mechanics*, 207,505-529.

[4] Sara Pratt. A Fresh Angle on Oil Drilling. *Geotimes*, March 2004.

[5] Frank M. White. *Fluid Mechanics.* McGraw Hill: 4th Edition, 1999.